Ab initio study of model guanine assemblies: The role of π-π coupling and band transport

Rosa Di Felice, Arrigo Calzolari, and Elisa Molinari

Istituto Nazionale di Fisica della Materia (INFM) and Dipartimento di Fisica, Università di Modena e Reggio Emilia,
Via Campi 213/A, 41100 Modena, Italy

Anna Garbesi

CNR ISOF, Area della Ricerca, Via P. Gobetti 101, 40129 Bologna, Italy

Several assemblies of guanine molecules are investigated by means of first-principles calculations. Such structures include stacked and hydrogen-bonded dimers, as well as vertical columns and planar ribbons, respectively, obtained by periodically replicating the dimers. Our results are in good agreement with experimental data for isolated molecules, isolated dimers, and periodic ribbons. For stacked dimers and columns, the stability is affected by the relative charge distribution of the π orbitals in adjacent guanine molecules. π-π coupling in some stacked columns induces dispersive energy bands, while no dispersion is identified in the planar ribbons along the connections of hydrogen bonds. The implications for different materials comprised of guanine aggregates are discussed. The band structure of dispersive configurations may justify a contribution of band transport (Bloch type) in the conduction mechanism of deoxyguanosine fibres, while in DNA-like configurations band transport should be negligible.

　　　　PACS number(s): 71.15.Mb, 73.22.Dj, 87.14.Gg

I. INTRODUCTION

The twofold issue of scaling down the electronic devices and of realizing a high circuit integration density on a single chip has recently seen a rise of the field of molecular electronics, which consists of the use of molecules to realize electrically conducting structures.[1,2] Because of their sequence-specific recognition properties, DNA molecules are attracting attention for the construction of nanometer scale devices, where they might be used, by virtue of their self-assembling capabilities, to wire the electronic materials in a programmable way.[3] This research path recently led to a set of controlled experiments for a direct measurement of the dc conductivity.

Using interdigital electrodes, anisotropic conductivity was found in an aligned DNA cast film: At room temperature, a large Ohmic current, linearly increasing with the applied voltage, was measured.[4] Ohmic behavior and high conductivity were also found, for a 600-nm-long rope made of a few λ-DNA molecules.[5] Instead, nonlinear current-voltage curves, exhibiting a voltage gap at low applied voltage, were measured through a single 10-nm-long poly(dG)/poly(dC) DNA molecule trapped between two metal nanoelectrodes.[6] Large currents were observed, in air and vacuum, both at ambient temperature and at 4 K. The authors suggested that the observed electron transport is best explained by a semiconductorlike band model where the electronic states are delocalized over the entire length of the base pair stack.[6]

The guanine (G) base is particularly interesting in view of obtaining conductive molecular aggregates, because of its low ionization potential, which suggests its viability to mediate charge motion along a sequence of bases.[7,8] This peculiar property has opened the way to the measurement of the electrical conductivity of G aggregates. Interestingly, a metallic nanogate, filled with a dried solution of a lipophilic derivative of 2'-deoxyguanosine,[9,10] displayed a current-voltage behavior[11] similar to that of the semiconducting poly(G)/poly(C) sample.[6] Previous investigations showed that, in organic solvents, this molecule undergoes extensive self-assembly, mediated by H bonding among the guanine bases, to give ribbonlike aggregates that, upon drying, form fiber structures within which the guanine cores of the ribbons lie on parallel planes at a distance of about 3.4 Å.[12,13] While a direct comparison among the findings for the deoxyguanosine materials and for DNA cannot be made, because of the different overall experimental settings and chemical nature of the molecules, one cannot avoid to notice the similar and peculiar current-voltage characteristics of the nanogates interconnected by molecules featuring self-assembled[9,10] or inherent[6] guanine stacks.

In the following, we have chosen to perform *ab initio* calculations of the structural and ground state electronic properties of extended model structures whose building block is the G base alone. Of course, we are well aware that these model structures are only partially related to the structure of a poly(G)/poly(C) duplex,[6] where each guanine is H bonded to a cytosine in the opposite strand. However, self-assembled G structures are among the simplest base aggregates characterized experimentally,[10,12] thus allowing accurate theoretical calculations as well as comparison with experimental data. Additionally, our choice is motivated by the role played by guanine, the DNA base with the lowest ionization potential, in the mechanism of charge transport.[14–16]

The main question that we address here is whether the electronic properties of extended G-based structures can account for a band-like mechanism for charge transport. Previous theoretical studies for DNA bases and for their assemblies can be found in the existing literature.[17–22] Both MP2/ Hartree-Fock and density-functional-based calculations were performed in the past with localized basis sets (GAUSSIAN) to treat isolated guanines and small clusters of guanines.[17] Here

we focus on density-functional-based calculations using a plane-wave basis and *ab initio* pseudopotentials:[23] this technique should allow for a correct description of solid aggregates of G's, resembling those of long-range deoxyguanosine fibers, provided the single molecules and the clusters are well described. Before simulating the structures of our interest, which are planar ribbons and stacked sequences of G's, we check that our technique is well suitable to describe isolated G molecules as well as pairs of molecules in different (lateral or vertical) configurations. We then consider $(GG)_n$ vertical stacks, and $(GG)_n$ isolated and stacked periodic ribbons. We study the stability of different vertical configurations as a function of the relative atomic positions between adjacent G molecules, and identify the role of π-π coupling. We demonstrate that pseudopotential plane-wave density-functional-theory (DFT) calculations at the current level of accuracy are able to reproduce not only the equilibrium length of isolated hydrogen bonds, but also periodic sequences of such bonds. Concerning the electronic properties, all the model solids that we considered are semiconducting with large energy gaps. The dispersion of the highest valence and lowest conduction bands is always negligible in the (x,y) plane containing the molecules (the guanines are connected laterally by H bonds). Conversely, the dispersion along the z direction perpendicular to the G planes is found to be extremely sensitive to the detailed geometric stacking of the bases, which in turn can be affected by different environments. In vertical stacking geometries that are similar to those present in DNA, the calculated dispersion of both the valence-band maximum and conduction-band minimum are extremely small. Consequently, both electrons and holes introduced by "doping" or photoexcitation would have very large effective masses—hence low mobility—in these types of structures. Instead, our results show that a bandlike contribution may be responsible for the conduction mechanism in the 2'-deoxyguanosine lipophilic derivative.[10]

The paper is organized as follows. Section II describes the computational method. Section III deals with the calculated equilibrium geometries and the electronic structure for the isolated G molecule and for the model guanine assemblies. Section IV presents a discussion of our results with an outlook to the implications for the physics of guanine ribbons and DNA-like stackings. Finally, Sec. V contains a summary of the arguments presented in the paper.

II. METHOD

Our calculations are based on the DFT in the local-density approximation (LDA).[24] For the hydrogen-bonded pairs and ribbons, we take into account BLYP gradient corrections to the exchange-correlation functional.[25] The electron-ion interaction is described via *ab initio* norm-conserving pseudopotentials in the factorized form of Kleinman and Bylander.[26] The search for optimized metastable structures is performed by total-energy minimizations with respect to the ionic and electronic degrees of freedom. The former are represented by the ionic coordinates, and the latter by the electronic wave functions. The ions are treated in a classical formalism, and are displaced according to the forces derived from the poten-
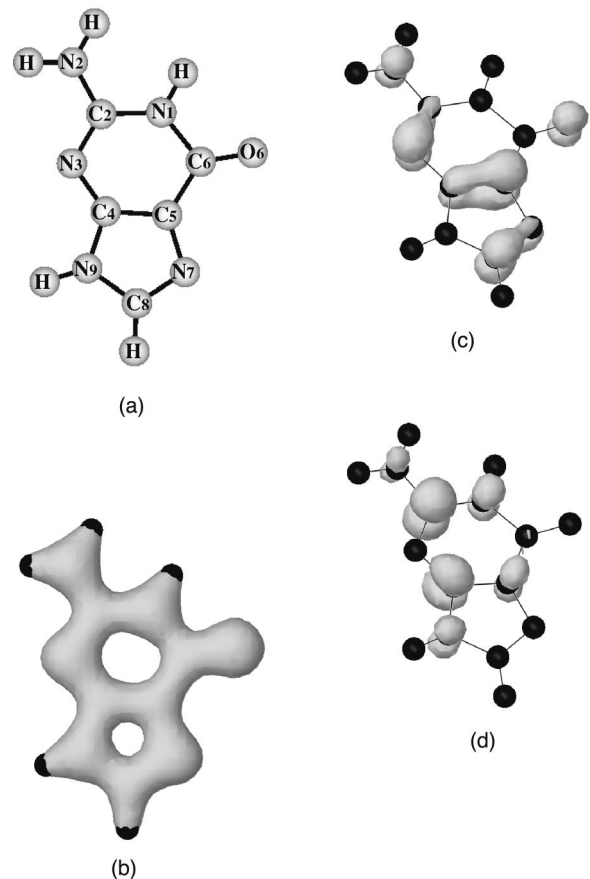

FIG. 1. (a) Planar view of the isolated guanine molecule, with indication of the chemical species. (b) Isosurface plot of the total charge density from the *ab initio* calculation. (c) Isosurface plot of the HOMO. (d) Isosurface plot of the LUMO.

tial determined by the full quantum-mechanical electronic structure,[23] within a Car-Parrinello-like scheme.[27] For any selected geometry, all the atoms are allowed to relax, until the forces vanish within an accuracy of 0.05 eV/Å. Thus, for each metastable structure, we obtain both the geometry and the consistent single-particle electron energies and wave functions. The electron wave functions are expanded in a basis of plane waves with kinetic energy up to 50 Ry. This cutoff is very high with respect to standard first-principle calculations for most solids, and is due to the presence of the first-row elements C, N, and O, whose valence electron wave functions have strong oscillations in the region around the nucleus, thus needing many plane waves for an accurate treatment. For one of the model systems, we have verified that increasing the precision of the calculations in both the plane-wave kinetic-energy cutoff (up to 60 Ry) and in the accuracy within which the atomic forces vanish (0.025 eV/Å), gives changes of the bond lengths smaller than 0.01 Å and of the bond angles smaller than 0.5°, within a guanine molecule, whereas the interplanar distance in the stacks is not affected at all. Additionally, for the diatomic molecules N_2 and O_2 the employed pseudopotential was tested up to a cutoff of 80 Ry, with no significant improvement.

Our method employs periodic boundary conditions in three dimensions. In order to simulate isolated molecules, we

TABLE I. Structural data for the isolated guanine molecule. The experimental structure taken from Ref. 31 and 32 is that for guanosine, with a sugar moiety instead of an H atom in position 9 (e.g., attached to atom N_9 in Fig. 1).

Distance (Å)			Angle (°)		
this work	experiment	discrepancy (%)	this work	experiment	discrepancy (%)
$(C_8\text{-}N_7)$ 1.281	1.304	−1.8	$(N_9C_8N_7)$ 112.4	113.5	−1.0
$(C_5\text{-}N_7)$ 1.347	1.389	−3.0	$(C_8N_7C_5)$ 105.5	104.2	+1.2
$(C_5\text{-}C_6)$ 1.419	1.415	+0.3	$(N_7C_5C_4)$ 110.6	110.8	−0.2
$(C_6\text{-}O_6)$ 1.186	1.239	−4.3	$(N_7C_5C_6)$ 130.8	130.1	+0.5
$(C_6\text{-}N_1)$ 1.415	1.393	+1.6	$(C_4C_5C_6)$ 118.6	119.1	−0.4
$(C_2\text{-}N_1)$ 1.345	1.375	−2.2	$(C_5C_6O_6)$ 131.4	128.3	+2.4
$(C_2\text{-}N_2)$ 1.336	1.341	−0.4	$(C_5C_6N_1)$ 109.2	111.7	−2.2
$(C_2\text{-}N_3)$ 1.287	1.327	−3.0	$(O_6C_6N_1)$ 119.4	120.0	−0.5
$(C_4\text{-}N_3)$ 1.323	1.355	−2.4	$(C_6N_1C_2)$ 127.1	124.9	+1.8
$(C_4\text{-}C_5)$ 1.383	1.377	+0.5	$(N_1C_2N_3)$ 122.6	124.0	−1.1
$(C_4\text{-}N_9)$ 1.346	1.377	−2.3	$(N_1C_2N_2)$ 117.0	116.3	+0.6
$(C_8\text{-}N_9)$ 1.361	1.274	−1.0	$(N_2C_2N_3)$ 120.3	119.7	+0.5
			$(C_2N_3C_4)$ 113.9	111.8	+1.9
			$(N_3C_4C_5)$ 128.5	128.4	+0.1
			$(N_3C_4N_9)$ 126.0	126.0	0.0
			$(C_5C_4N_9)$ 104.6	105.6	−0.9
			$(C_4N_9C_8)$ 107.0	106.0	+0.9

choose a large supercell of size $15.9 \times 15.9 \times 10.6$ Å^3. Such a choice ensures that the minimum distance (in any spatial direction) between two molecules is larger than 8.5 Å. In particular, the distance is 10.6 Å in the direction perpendicular to the plane of the molecules, very large with respect to the distance of 3.37 Å between two neighboring bases in B-DNA. The supercells for different assemblies of G molecules are described in Sec. III, where the model structures are discussed in detail. For Brillouin-zone sums, the single high-symmetry Γ point has been employed in the case of isolated molecules and dimers, while one or two (depending on the symmetries) special **k** points[28] have been employed in the case of periodic columns and ribbons, and in the case of stacked ribbons.

The computational technique has been successfully applied in many investigations of the structure and electronic properties of inorganic and organic materials.[24,29,30] In Sec. III, before reporting the results of our calculations for the model guanine assemblies, we address the issue of extending such calculations to biomolecules, by presenting a test on the G base.

III. RESULTS

In this section we present our results for isolated G molecules and their assemblies, and discuss them in the framework of the existing theoretical literature, which is limited to isolated G's and G pairs[18−20] and does not give any account of periodic G columns and ribbons. We relate the outcome of the calculations to new experimental findings about the structure and electrical behavior of deoxyguanosine-based solids.[10]

The section is divided into subsections for different systems: (A) an isolated G molecule, (B) stacked GG dimers, (C) stacked $(GG)_n$ columns, (D) hydrogen-bonded GG pairs, and (E) hydrogen-bonded $(GG)_n$ ribbons and stacked ribbons.

A. Isolated guanine molecule

We start by presenting the calculated structure and selected electron states for the G molecule. This simple system allows us to evaluate the accuracy of our method, by comparison with x-ray data and with the outcome of previous *ab initio* calculations. Furthermore, the total energy of the equilibrium structure of the isolated molecules is necessary in order to evaluate formation energies of dimers, ribbons, and columns.

The structure of guanine is well known from x-ray studies.[31,32] Figures 1(a) and 1(b) show a plane view of the molecule, and the isosurface plot for the total charge density. The calculated bond lengths and angles are in good agreement with x-ray data (see Table I). Most of the bond lengths are *underestimated* within 2% and 3% with respect to the experimental structure, the only exceptions being the *underestimate* of 4.3% for the $C_6\text{-}O_6$ bond and the *overestimate* of 1.6% for the $C_6\text{-}N_1$ bond. The average C-H and N-H distances, not reported in Table I, are 1.08 and 1.01 Å, respectively, in good agreement with bond lengths in NH_3 and CH_3 molecules. The bond angles in guanine are also reproduced with a high degree of accuracy (Table I): the discrepancy with respect to the experimental data is below 2.5%, but the average percentage error is 1%. The formation energy of G, with respect to its elemental components in stable phases

(O_2, H_2, and N_2 molecules, crystalline diamond) is 87.5 Kcal/mole. By starting the atomic relaxation with a planar G molecule as the initial condition, we find that the planar configuration is indeed a metastable state. By considering a different initial condition with a non-planar amino group [the NH_2 complex bonded to the site C_2; see Fig. 1(a)], we find another metastable state. However, the deviation from planarity is small, and the total energy difference between the planar and the puckered geometries is also very small, within the precision of our calculations [estimated to be about 10 meV/G (Ref. 33)]. While previous calculations pointed out a stronger stabilization effect of nonplanarity,[19] no direct gas-phase experimental data exist. Moreover, the hydrogen bonds tend to flatten the structure when forming dimers and ribbons of G's; thus we are confident that our results for the periodic structures are not affected by this issue.

The single particle eigenvalues are characterized by a DFT-LDA energy gap of 4.8 eV between the highest occupied molecular-orbital (HOMO) and the lowest unoccupied molecular-orbital (LUMO) electron states.[24] We have identified σ and π orbitals. The HOMO [see Fig. 1(c)] has a π character and is localized on C_8, O_6, and N_2 atoms and C_4-C_5 and N_3-C_2 bonds. The LUMO [see Fig. 1(d)] has a π character and is localized on N_9, C_4, C_5, C_2, and N_1 atoms. Because they extend out of the guanine plane, both the HOMO and LUMO states are well suitable for interactions with adjacent similar states when forming vertical stacks, inducing a splitting of degenerate molecular orbitals by an amount that depends on the strength of such interactions. In the case of an infinite periodic stack, this is the mechanism that may give rise to band dispersion for sufficiently strong coupling, and to mobile carriers if the bands are partially occupied (for instance, as a consequence of doping or photoexcitation).

B. Stacked GG dimers

In order to select low-energy geometries for the vertical columnar structures, whose electronic properties are the main subject under investigation, we first considered stacked dimers. We name stacked dimer a pair of G molecules lying in parallel planes whose distance in the perpendicular direction is an output of our calculations. A column is obtained by periodically replicating a dimer along the stacking (perpendicular) direction.

We have analyzed several configurations (Fig. 2) characterized by the relative azimuthal rotation angle of the two G's in the pair, with respect to an axis perpendicular to the G plane, and by an in-plane translation. The supercell used in the calculations was $15.9 \times 15.9 \times 19.1$ Å.[3] With periodic boundary conditions, two dimers in neighboring supercells are 15.7 Å apart in the stacking direction, sufficient to avoid spurious interactions between them. By allowing all the atoms to relax, the interplanar distance between the two G's in a pair was a free parameter. In this way we determined the equilibrium interplanar distance to be used in the calculations for the periodic columns. For all the configurations shown in Fig. 2 (e.g., independently of the relative rotation angle between the bases), the average interplanar distance
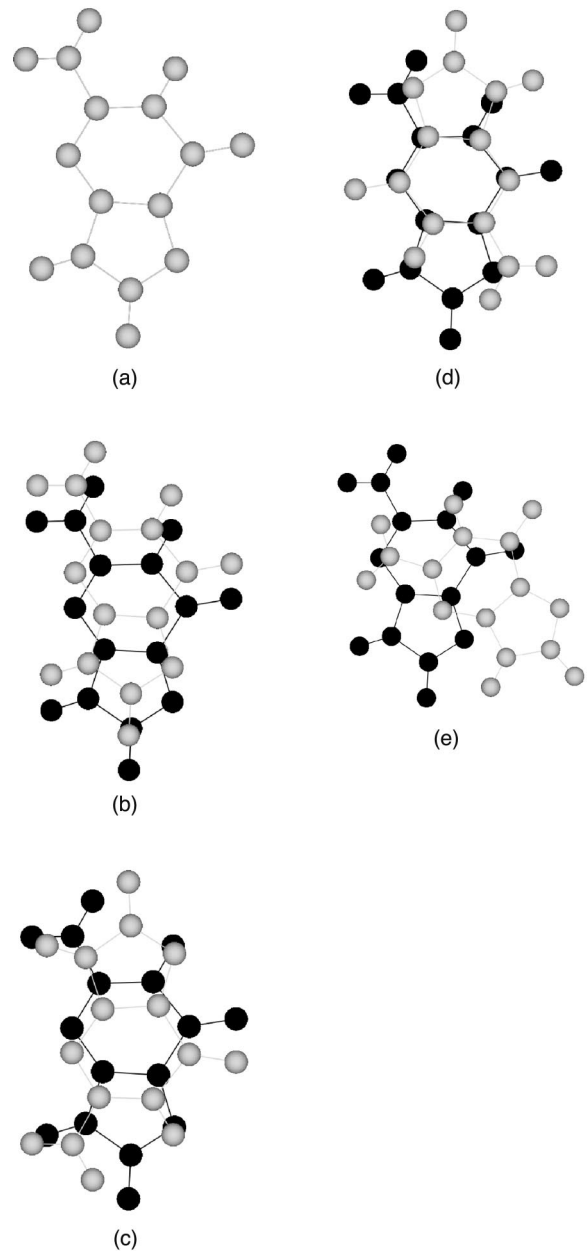

FIG. 2. Top views of different stacked dimer configurations. The structures are explicitly defined in the text. Gray (black) dots and lines are used to represent atoms and bonds in the upper (lower) plane. Columnar structures are obtained by replicating the dimer units along the direction perpendicular to the plane of the figure. The chemical species are read from Fig. 1(a).

was 3.37 Å, typical of base stacks in B-DNA. Each base maintained a planar geometry, with out-of-plane fluctuations smaller than 0.05 Å.

Top views of the computed stacked dimers are illustrated in Fig. 2. In Fig. 2(a), the two G's of the dimer are perfectly eclipsed, in particular the hexagonal rings are on top of each other, and there is maximum superposition of the π-like HOMO and LUMO of the two guanines (labeled GGv.A). In Fig. 2(b), the rotation angle is zero as for GGv.A, but the center of mass of one molecule is shifted with respect to the

other, in order to lower the π-π superposition (labeled GGv.B). In Fig. 2(c), the azimuthal rotation angle is zero, as well as the relative translation of the two G's, but there is a reflection of the upper molecule with respect to its plane: this configuration (labeled GGv.C) is the only one, among those considered in this work, that exhibits a reflection and allows to discriminate between two molecular faces. In Fig. 2(d), the rotation angle is 180°, and the π-π superposition is large, though smaller than in GGv.A (labeled GGv.D). In Fig. 2(e), the azimuthal rotation angle is 36°, and a translation brings the two molecules in a configuration similar to that in B-DNA (labeled GGv.E).

Although some of these stacked structures are not likely to occur in nature, they allow one to understand important microscopic features that may be relevant in real structures. Most notably, the dependence of the stability and of the electronic properties on the azimuthal angle and π superposition is accessible. The lowest-energy configuration among those shown in Fig. 2 is GGv.D, while GGv.A has the highest formation energy, and the other dimers have intermediate formation energies.[34] However, the energy difference between the two extreme cases GGv.A and GGv.D is small, about 250 meV/G. We attribute the highest formation energy of GGv.A to the electrostatic repulsion due to the complete π-π superposition. In fact, the π-like HOMO's of guanines in neighboring planes are mostly responsible for their interaction: the superposition of negative charge in the same region of space (the hexagonal ring) for configuration GGv.A contributes with a Coulomb repulsion. The π-π superposition is also large in GGv.D, but the repulsion is much smaller, making GGv.D a more viable model for a stacked GG pair.[18]

We wish to point out that, although the lower superposition of adjacent π orbitals of GGv.D with respect to GGv.A decreases the electrostatic repulsion between the two molecules and makes the dimer more viable, such interaction is still rather large and is the origin of energy dispersion in columnar structures based on the GGv.D dimer. This issue is addressed in Sec. III C, by computing the band structures of model periodic stacks built up with the dimers just described. It is also worth stressing that, for stacked dimers, without inclusion of sugars, phosphates, and water as in real situations, the rotation angle of 36° is not preferred. This result is in line with the fact that the inner core of the base pair stack is not completeley responsible for the stability of double-stranded DNA, but also the backbone and the environment are relevant factors.

C. Periodic stacked poly(G) columns

The building block of each periodic stack is a GG pair; we have analyzed five different model columns starting from the dimers described above (Fig. 2). The supercell for these calculations is $15.9 \times 15.9 \times 6.74$ Å^3: no vacuum region separates two adjacent dimers in the stacking direction. The periodic structures are labeled with the same names as the stacked dimers. Direct and reciprocal one-dimensional crys-

TABLE II. Energetic and electronic data of different periodic stacked configurations. E_{form}^1 is calculated with respect to the N_2, O_2, and H_2 molecules, and C in the diamond phase. E_{form}^2 is calculated with respect to isolated guanine molecules. E_{gap} is the energy difference between the HOMO and LUMO single particle eigenstates, calculated by DFT-LDA (Ref. 24). $m_e(m_h)$ is the electron (hole) effective mass, in units of the free electron mass m_0. The structures are labeled as in Fig. 2; G is a single molecule.

	G	GGv.A	GGv.B	GGv.C	GGv.D	GGv.E
E_{form}^1 (eV/G)	−3.80	−3.69	−3.79	−3.93	−4.07	−3.89
E_{form}^2 (meV/G)	0	+100	0	−130	−280	−100
E_{gap} (eV)	4.8	2.97	3.71	4.12	3.63	3.54
m_e (m_0)		1.41			2.80	∞
m_h (m_0)		1.04			2.20	5.25

tal lattices are associated with the periodic columns: the basis vectors of these lattices are $\mathbf{a}_3 = 6.74$ Å and $\mathbf{b}_3 = (2\pi/a_3)\hat{a}_3$.

The formation energies are reported in Table II. The energetical order is the same as for the dimers. The most stable configuration is GGv.D. We stress again that configuration A, with a very large π-π superposition, has the highest formation energy. The energy is substantially reduced in the column GGv.D, where the superposition is still large but the repulsion is weaker: the hexagonal rings lie on top of each other, but the O atoms in adjacent planes lie opposite to each other. Thus we attribute the dominant repulsive contribution of the π-π interaction to the O atoms.

A detailed analysis of the electronic properties reveals other interesting features. We report the numerical data in Table II, and we show the bandstructure for columns GGv.A, GGv.D, and GGv.E in Fig. 3.

GGv.E, with the two G's rotated by 36° as in portions of nucleic acids, has flat HOMO- and LUMO-derived bands, very large effective masses, and is therefore incompatible with even a partial band transport mechanism for the conduction in guanine-based devices.[10] The periodic columns GGv.A and GGv.D, instead, have electronic properties that may support electronic transport through the base stack. For GGv.A, the HOMO band disperses downward by 0.65 eV and the LUMO band disperses upward by 0.52 eV, between the center (Γ) and the edge ($A = \frac{1}{2}\mathbf{b}_3$, $\mathbf{b}_3$ being the reciprocal lattice vector along the stacking direction) of the Brillouin zone. For GGv.D, the dispersions of the HOMO and LUMO bands are, respectively, 0.26 eV downward and 0.13 eV upward. The effective masses of GGv.A and GGv.D, reported in Table II, are of the order of 1–2 free-electron masses. Although these values are much larger than those of conducting organic polymers,[35] they are similar to those of inorganic materials for which band transport is demonstrated. Notable examples of such materials are wide-bandgap semiconductors, such as group-III nitrides.[36] As a note to support the strength of our results, we wish to point out that a test calculation for the model GGv.A demonstrates that the values of the band dispersions do not depend (within 0.02 eV) on the accuracy required for vanishing atomic forces (0.025
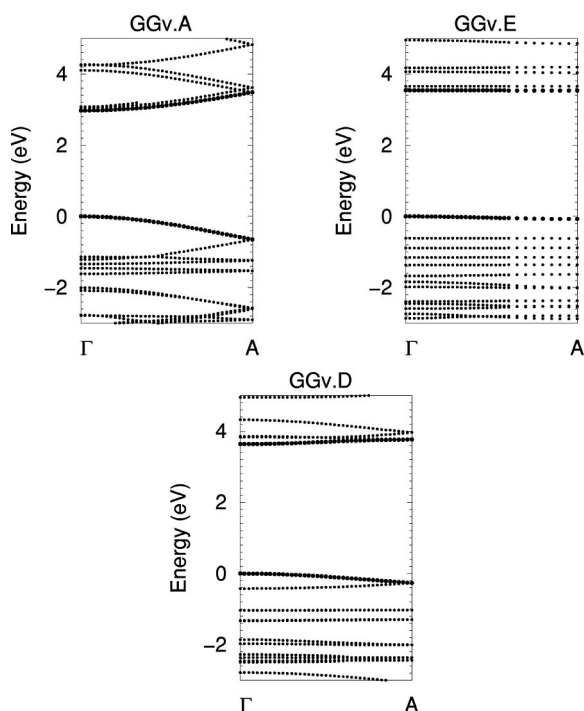
FIG. 3. Band structure for configurations GGv.A, GGv.D, and GGv.E, calculated along the symmetry line parallel to the stacking direction. Larger dots indicate HOMO and LUMO states. The single-particle energies reported in these plots are relative to the top of the highest valence band.

eV/Å instead of 0.05 eV/Å), and to the approximation employed for the exchange-correlation functional (BLYP instead of LDA).

To illustrate how the π-π stack may originate channels for charge migration through a band transport mechanism, in Fig. 4 we show an isosurface of the HOMO state at the A point for the columnar structure GGv.D: the interaction between the two molecules in the cell is evident in the superposition resulting in a delocalized orbital.

Summarizing our study of the columnar structures, we emphasize that the orbital interaction is strong. At variance, we will soon show that it is practically absent in hydrogen-
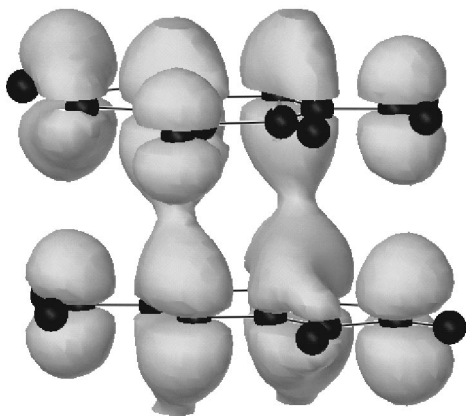

FIG. 4. Isosurface plot of the HOMO state at point A for the columnar structure GGv.D.
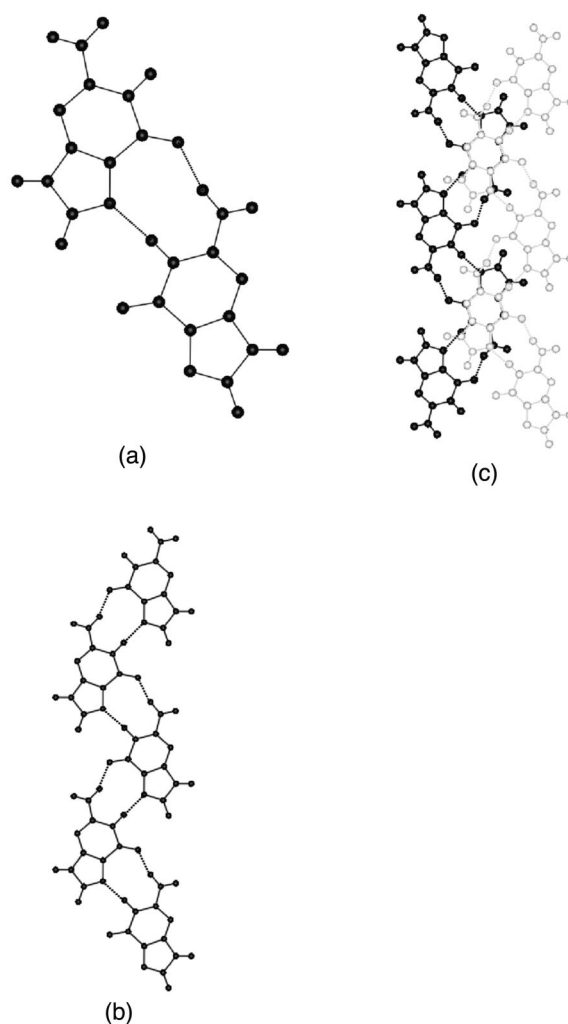

FIG. 5. (a) Top view of the hydrogen-bonded GG dimer. (b) Top view of the hydrogen-bonded ribbon obtained by periodically replicating the dimer, also representing the structure SR.A for the stacked ribbons. (c) Top view for the stacked ribbon structure SR.D. Black and gray dots identify atoms lying in two different parallel planes.

bonded pairs. This is in agreement with the common knowledge that hydrogen bonds have an electrostatic (rather than covalent) nature. In the following subsections, we compare the behavior of planar G pairs and ribbons with that of stacked G pairs and columns. In particular, we find that hydrogen bonding does not give origin to dispersive electron bands, contrary to what we have seen for the π stacking.

D. Planar hydrogen-bonded GG dimers

We have selected one possible arrangement of hydrogen bonds, giving a structure named GG3 [Fig. 5(a)][17,21]. We have not considered other documented hydrogen-bonded GG pairs,[17] because we focus our interest here in the guanine ribbons present in the fibers of a lipophilic derivative of 2'-deoxyguanosine: Such fibers[13] have the bond network illustrated in Fig. 5(b). The equilibrium structure that we obtain after atomic relaxation is in good agreement with that of

TABLE III. Energetic and electronic data of isolated and stacked ribbons, as defined in Table II.

	Ribbon	SR.A	SR.D
E_{form}^2 (meV/G)	−820	−310	−580
E_{gap} (eV)	3.84	2.61	3.12
$m_e(m_0)$		1.24	∞
$m_h(m_0)$		1.07	2.05

the GG3 hydrogen-bonded pair previously described via quantum chemistry and DFT cluster calculations.[17] The two individual G molecules in the planar pair remain very similar to their isolated form. The N7(H)···N1 hydrogen bond has a length of 2.93 Å, and forms an angle of 177° (2.96 Å and 173° in the theoretical literature[17]). The N2(H)···O6 hydrogen bond has a length of 2.85 Å and forms an angle of 169° (3.27 Å and 166° in the theoretical literature[17]). Our calculated value for the DFT-BLYP energy gap[24] of the GG3 dimer is 2.45 eV. The formation energy of the structure, with respect to two isolated guanine molecules, is -310 meV/G. This value, compared to the formation energy of the most stable stacked dimer GGv.D ($\simeq -200$ meV/G), is in agreement with the previous demonstration that hydrogen bonds are stronger than stacking interactions.[17]

The structure of the GG3 dimer was calculated only as a basic building block of the fiber-state ribbons, whose electronic properties we are interested in. Thus we believe that the underestimate of the N2(H)···O6 distance with respect to the results of other computations is not a serious issue. A slight underestimate of the hydrogen-bonds calculated in the framework of DFT is documented.[17] Furthermore, the contraction of the N2(H)···O6 hydrogen bridge is due to an imprecise account of secondary interactions such a as C8(H)···O6. It is likely that such a secondary interaction is reduced in one-dimensional ribbons, thus minimizing the shortcomings of DFT.

E. Planar hydrogen-bonded ribbons

In a periodic ribbon obtained by piling up replicas of the GG3 dimer [Fig. 5(b)], the equilibrium structure maintains the bonding characteristics of the dimer. There is a huge energy gain in forming the one-dimensional ribbon, of 820 meV/G with respect to isolated G molecules, and of 510 meV/G with respect to the hydrogen-bonded GG3 pair (Table III). Note that G has a large dipole moment;[19] the dipole moments of G's add up to give a nonvanishing dipole also in the GG3 dimer and in the ribbon, parallel to the ribbon axis.[10] Such electrostatic interactions account for the high stability of the planar hydrogen-bonded structures, well known both in solution and in the solid state.

The band structure of the ribbon was calculated along a symmetry line parallel to its axis. The HOMO- and LUMO-derived bands are separated by a DFT-BLYP energy gap[24] of 3.84 eV, and are both dispersionless. Consequently, these bands have practically infinite effective masses, so that the electrons and holes in these states are not mobile according to this picture. The electronic state analysis shows that the

HOMO and LUMO have a π character, similar to isolated G. The electronic states are localized around single G molecules, no delocalized intermolecular states, extended through the hydrogen bonds in the ribbon, are present. The dispersion induced by hydrogen bonding is not compatible with band transport. The only possible conduction mechanism through hydrogen bonds is via electrostatic interactions. Therefore, in a device where dried deoxyguanosine fibers are deposited between two metal electrodes,[10] if just one planar layer of ribbons is formed between the electrodes, band transport cannot contribute to conduction.

In order to investigate the competition of π-π coupling versus hydrogen-bonding interactions, we have simulated two different configurations of stacked ribbons, periodic along the stacking direction. Top views are shown in Figs. 5(b) and 5(c). Figure 5(b) indeed shows a single ribbon, but the top view is equivalent for two exactly eclipsed ribbons on top of each other (label SR.A): the stacking between adjacent bases is similar to that of column GGv.A, and all the individual bases are perfectly aligned. Figure 5(c) shows a stack of two ribbons where only half of the individual G molecules lie on top of each other, with a stacking similar to that of configuration GGv.D (this structure is labeled SR.D). In both the SR.A and SR.D geometries, the projections of the ribbon axes on the (x,y) plane coincide, identifying an axis for the stack: this axis defines the $\Gamma - X$ direction in the one dimensional Brillouin zone.

The supercells are $21.2 \times 11.3 \times 6.74$ Å^3 for SR.A and $24.3 \times 11.3 \times 6.74$ Å^3 for SR.D. The choice of different supercells allows one to have a vacuum region of the same volume between neighboring ribbons in the two configurations SR.A and SR.D. The relaxed structures maintain the geometry of the single ribbon: no G deformations, no variations of H-bond lengths and angles, and no out-of-plane buckling are observed. This finding indicates that the stacking does not affect the hydrogen-bonding mechanism that determines the structure of the isolated ribbon.

Numerical data for the energetics and the electronic properties are reported in Table III. Both SR.A and SR.D structures are energetically favorable with respect to isolated G molecules and to stacked columns, but unfavorable with respect to isolated ribbons, as indicated by the smaller energy gain of the stacked ribbons. Configuration SR.D is more stable than SR.A by 280 meV: this trend is consistent with what found previously for the columnar stacks, where a higher stability is achieved by lowering the π-π superposition in building the stacks. Although configurations SR.A and SR.D, which we calculate here, are not viable models for piling up ribbons into solid-state crystals, ordered phases for deoxyguanosine fibers are known to exist.[12] We note that other factors, such as the presence of the phosphate-sugar backbone, or the possibility of different relative positions of the neighboring ribbons, should be taken into account to achieve a full description, which is beyond the scope of this work.

In Fig. 6 we show the calculated bandstructure for the SR.A and SR.D configurations. In both cases, the HOMO- and LUMO-derived bands are dispersionless along the Γ-X
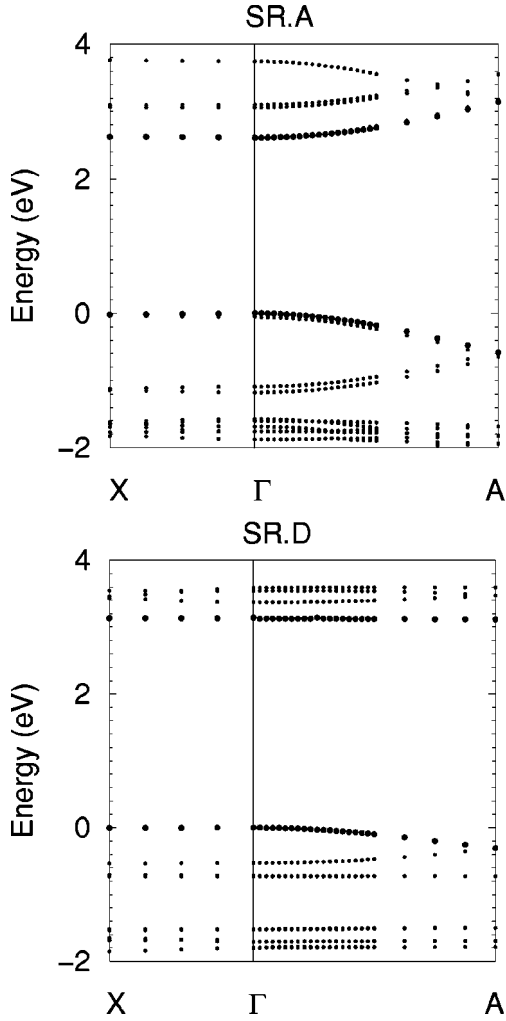
FIG. 6. Band structure for configurations SR.A and SR.D, calculated along the symmetry lines parallel to the ribbon direction ($\Gamma - X$) and to the stacking direction (Γ-A). Large dots indicate HOMO and LUMO states.

direction, and the charge carriers are not mobile in this direction. This behavior is the same as in isolated ribbons: therefore, it is further evidence that the base-base interactions due to the stacking do not change the features of the ribbons. In the Γ-A direction, parallel to the stacking direction, the HOMO- and LUMO-derived bands are dispersive, as in the columnar structures of Sec. III C.

The bands for structure SR.A in the Γ-A direction are more dispersive than those for structure SR.D, due to the higher π-π superposition. As a consequence, the corresponding electron and hole effective masses along the Γ-A direction are smaller. The effective masses of the stacked-ribbon periodic structures are very similar to those of the stacked periodic columns (Sec. III C): this is an indication that the hydrogen-bonding network of the individual ribbons does not affect the electronic properties in the perpendicular direction. The only exception to this trend is m_e, which becomes infinite for the stacked ribbons SR.D while it is finite for the equivalent stacked column GGv.D: this is due to the fact that in structure SR.D one-half of the individual bases

are on top of each other [see Fig. 5(c)], while the other half do not participate in the π-π coupling.

Summarizing the results discussed above, we wish to point out that the π-π coupling and H bonding interaction mechanisms are not in competition. H-bonding has an electrostatic nature and accounts for in-plane stabilization: it is not compatible with a band transport mechanism, and it is not modified by base stacking. π-π coupling is weaker than H bonding: it is compatible with band transport along the stacking direction and it is not affected by the local details of the planar base sequence.

IV. DISCUSSION

A. Guanosine films

As outlined in Sec. I, the recent lively research activities in molecular electronics have pointed out peculiar guanine assemblies to be exploited as electrical conductors. In fact, experiments on a lipophilic derivative of 2'-deoxyguanosine[10] demonstrated conduction through the biomolecular material deposited in a nanogate between metal electrodes. The details of the conductivity depend on the experimental conditions, in particular on the gate width. Our results indicate that the observed conductivity, resembling that of a semiconductor in the intermediate gate length regime (a few hundred nm) and that of a diode junction in the short gate length regime (less than 100 nm), is compatible with a Bloch contribution to the transport mechanism. We have shown that delocalized orbitals through the base stack may be formed, provided that a relevant superposition of the hexagonal rings of the single guanines is maintained. Therefore, if the guanosine ribbons in the device gate align locally with their plane perpendicular to the direction connecting the electrodes, in a geometry similar to that proposed as SR.A, then extended Bloch-like states may be partially responsible for the observed conduction. This stacking orientation does not need to be complete in order for the proposed mechanism to work: it is sufficient that randomly aligned stacks form locally, and that the total resulting component in the direction connecting the electrodes is non vanishing. In a gate length regime ranging from 100 to 300 nm, semiconductinglike conductivity is revealed: we propose that, in such a condition, the ribbons are locally stacked in such a way to form partially delocalized orbitals that give a global band-like contribution. In the gate length regime below a 100 nm, a diode-like behavior is observed: this characteristic is assigned to an interaction of the π stack with the total dipole moment of the ribbons, as discussed elsewhere.[10]

B. DNA molecules

While our study is limited to a single type of nucleoside, it also allows a discussion of the electronic properties of DNA molecules, where G sequences in base stacks play an important role.[37,38,15] Depending on the energetics of the base sequence, and on the overall structural aspects of the system under investigation, the mechanisms proposed for DNA-mediated charge migration include single-step super-

exchange,[39,40] multistep hole hopping,[8,14] phonon-assisted polaron hopping,[15] and band transport.[6]

In DNA double strands, the relative arrangement of neighboring bases along the axis of the helix[31] is characterized by a rotation angle around 36°. Our results show that periodic G columns in such a configuration do not support the formation of extended molecular orbitals. Therefore, band transport would not be effective. For what concerns the mechanism of conductivity in DNA molecules, our results support the conclusion that the contribution of band transport would be very small,[41,14,42] in contrast to recently proposed interpretations of experimental data,[6] unless structural distortions, possibly activated by temperature effects, may induce rotations that support the formation of partially delocalized electron states. Although in real DNA molecules the backbone phosphate and sugar groups may affect the overall charge mobility, we believe that the presence of the outer mantle would not change our present conclusion that band transport is not supported by the native DNA stack: eventually, it may contribute a hopping or ionic mechanism, but it is unlikely to contribute to the formation of extended electron orbitals. The importance of the base stack for electron transfer through DNA molecules was highlighted in recent theoretical invesigations.[41]

V. CONCLUSIONS

We have reported the results of *ab initio* calculations for the structure, energetics, and electronic properties of several guanine assemblies. The geometry of isolated molecules and hydrogen-bonded dimers is well described with our technique, based on plane-wave pseudopotential density-functional theory, as demonstrated by comparison to available theoretical and experimental data.

We found that hydrogen bonding and π-π coupling are independent mechanisms that control the self-assemblying of guanine bases. Hydrogen bonding is not responsible for band transport: In fact, we have shown that no band dispersion is present along a planar ribbon of H-bonded guanines. Instead, base stacking is accompanied by π-π interactions that, for the case of sufficiently large overlap between adjacent π orbitals (e.g., the GGv.D configuration), induce energy dispersion and are consistent with charge mobility. Therefore, band transport may be partially responsible for charge mobility in nucleotide aggregates, in structures characterized by a large base-base superposition. This mechanism is likely complemented by hopping to connect (through space) different regions where such superposition is realized.

[1] A. Aviram and M. Ratner, Ann. N.Y. Acad. Sci. **852**, (1998).

[2] C. Joachim, J. K. Gimzewski, and A. Aviram, Nature (London) **408**, 541 (2000).

[3] E. Braun, Y. Eichen, U. Sivan, and G. Ben-Yoseph, Nature (London) **391**, 775 (1998).

[4] Y. Okahata, T. Kobayashi, K. Tanaka, and M. Shimomura, J. Am. Chem. Soc. **120**, 6165 (1998).

[5] H.-W. Fink and C. Schönenberger, Nature (London) **398**, 407 (1999).

[6] D. Porath, A. Bezryadin, S. de Vries, and C. Dekker, Nature (London) **403**, 635 (2000).

[7] E. Meggers, M. E. Michel-Beyerle, and B. Giese, J. Am. Chem. Soc. **120**, 12950 (1998).

[8] J. Jortner, M. Bixon, T. Langenbacher, and M. E. Michel-Beyerle, Proc. Natl. Acad. Sci. U.S.A. **95**, 12759 (1998).

[9] R. Rinaldi, E. Branca, R. Cingolani, S. Masiero, G. P. Spada, and G. Gottarelli, Appl. Phys. Lett. **78**, 3541 (2001).

[10] R. Rinaldi *et al.*, arXiv: cond-mat/0006402 (unpublished); and (unpublished).

[11] It is worth stressing that, in the experiment on deoxyguanosine, neither the polyanionic phosphate backbone that connects the nucleoside moieties in DNA nor the necessary counterions are present. Therefore, conduction through the bases is directly evaluated.

[12] G. Gottarelli, S. Masiero, E. Mezzina, G. P. Spada, P. Mariani, and M. Recanatini, Helv. Chim. Acta **81**, 2078 (1998).

[13] G. Gottarelli, S. Masiero, E. Mezzina, S. Pieraccini, J. P. Rabe, P. Samorí, and G. P. Spada, Chem. Eur. J. **6**, 3242 (2000).

[14] M. Bixon, B. Giese, S. Wessely, T. Langenbacher, M. E. Michel-Beyerle, and J. Jortner, Proc. Natl. Acad. Sci. U.S.A. **96**, 11713 (1999).

[15] G. B. Schuster, Acc. Chem. Res. **33**, 253 (2000).

[16] B. Giese, Acc. Chem. Res. **33**, 631 (2000); K. Nakatani, C. Dohno, and I. Saito, J. Am. Chem. Soc. **122**, 5893 (2000).

[17] J. Šponer, J. Leszczynski, and P. Hobza, J. Phys. Chem. **100**, 1965 (1996).

[18] J. Šponer, J. Leszczynski, and P. Hobza, J. Phys. Chem. **100**, 5590 (1996).

[19] P. Hobza, and J. Šponer, Chem. Rev. **99**, 3247 (1999), and references therein.

[20] H. Sugiyama and I. Saito, J. Am. Chem. Soc. **118**, 7063 (1996).

[21] M. Machado, P. Ordejon, E. Artacho, D. Sanchez-Portal, and J. M. Soler, physics/9908022 (unpublished).

[22] J. Hutter, P. Carloni, and M. Parrinello, J. Am. Chem. Soc. **118**, 8710 (1996).

[23] M. Bockstedte, A. Kley, J. Neugebauer, and M. Scheffler, Comput. Phys. Commun. **107**, 187 (1997)

[24] R. M. Dreizler and E. K. U. Gross, *Density Functional Theory. An Approach to the Quantum Many-Body Problem* (Springer-Verlag, Berlin, 1990). This book also discusses the well-known underestimate of the bandgap energies that is characteristic of DFT in the different approximations that are commonly adopted.

[25] A. D. Becke, Phys. Rev. A **38**, 3098 (1988); C. Lee, W. Yang, and R. C. Parr, Phys. Rev. B **37**, 785 (1988).

[26] N. Troullier and J. L. Martins, Phys. Rev. B **43**, 1993 (1991); L. Kleinman and D. M. Bylander, Phys. Rev. Lett. **48**, 1425 (1982).

[27] R. Car and M. Parrinello, Phys. Rev. Lett. **55**, 2471 (1985).

[28] H. J. Monkhorst and J. D. Pack, Phys. Rev. B **13**, 5188 (1976).

[29] For a review on the surfaces of inorganic materials, see, e.g., C. M. Bertoni, G. Roma, and R. Di Felice, *Electronic Structure of Adsorbates on Surfaces. Adsorption on Semiconductors*, edited by K. Horn and M. Scheffler, Handbook of Surface Science, Vol. 2 (Elsevier, Amsterdam, 2000), and references therein.

[30] E. Wimmer, *Density Functional Approaches for Molecular and Materials Design*, edited by B. B. Laird, R. B. Ross, and T. Ziegler, ACS Symposium Series Vol. 629 (American Chemical Society, Washington, DC, 1996), p. 423.

[31] W. Saenger, *Principles of Nucleic Acid Structure* (Springer-Verlag, New York, 1984).

[32] R. Taylor and O. Kennard, J. Mol. Struct. **78**, 1 (1988).

[33] The unit eV/G that we use here for the formation energies means eV per guanine molecule. The conversion factor is 1 eV/G =23.25 Kcal/mole.

[34] The fact that the dimer GGv.C (the only structure in which one molecule is reflected) is not energetically favorable with respect to other geometries indicates that the two faces of guanine are inequivalent for what concerns the stacking properties.

[35] P. Gomes Da Costa and E. M. Conwell, Phys. Rev. B **48**, 1993 (1993).

[36] S. K. Pugh, D. J. Douglas, S. Brand, and R. A. Abram, Semicond. Sci. Technol. **14**, 23 (1999).

[37] M. W. Grinstaff, Angew. Chem. Int. Ed. Engl. **38**, 3629 (1999).

[38] P. F. Barbara and E. J. C. Olson, Adv. Chem. Phys. **107**, 647 (1999).

[39] F. D. Lewis, T. Wu, X. Liu, R. L. Letsinger, S. R. Greenfield, S. E. Miller, and M. R. Wasielewski, J. Am. Chem. Soc. **122**, 2889 (2000).

[40] This is the basic mechanism for electron-hole transfer through tunneling between localized molecular states [R. A. Marcus and N. Sutin, Biochim. Biophys. Acta **811**, 265 (1985)].

[41] Y.-J. Ye, R.-S. Chen, A. Martinez, P. Otto, and J. Ladik, Solid State Commun. **112**, 139 (1999); Y.-J. Ye and Y. Jiang, Int. J. Quantum Chem. **78**, 112 (2000).

[42] P. J. de Pablo, F. Moreno-Herrero, J. G. Herrero, P. Herrero, A. M. Baró, P. Ordejon, J. M. Soler, and E. Artacho, Phys. Rev. Lett. **85**, 499 (2000).